Journal of General Virology (2014), **95**, 1770–1782 **DOI** 10.1099/vir.0.066829-0

Disintegrin-like domain of glycoprotein B regulates Kaposi's sarcoma-associated herpesvirus infection of cells

Lia R. Walker, Hosni A. M. Hussein and Shaw M. Akula

Department of Microbiology and Immunology, Brody School of Medicine at East Carolina University, Greenville, NC 27834, USA

Correspondence
Shaw M. Akula
akulas@ecu.edu

Kaposi's sarcoma-associated herpesvirus (KSHV) glycoprotein B (gB) is a lytic structural protein expressed on the envelope of mature virions and on the membrane of cells supporting lytic infection. In addition to this viral glycoprotein's interaction with integrins via its RGD (Arg-Gly-Asp) motif, KSHV gB possesses a disintegrin-like domain (DLD), which binds integrins as well. Prior to this study, there has been minimal research involving the less common integrin-binding motif, DLD, of gB as it pertains to herpesvirus infection. By using phage display peptide library screening and molecular biology techniques, the DLD of KSHV gB was shown to interact specifically with non-RGD binding $\alpha 9\beta 1$ integrins. Similarly, monitoring wild-type infection confirmed $\alpha 9\beta 1$:DLD interactions to be critical to successful KSHV infection of human foreskin fibroblast (HFF) cells and human dermal microvascular endothelial cells (HMVEC-d) compared with 293 cells. To further demonstrate the importance of the DLD of gB in KSHV infection, two recombinant virus constructs were generated using a bacterial artificial chromosome (BAC) system harbouring the KSHV genome (BAC36): BAC36ΔD-KSHV (lacking a functionally intact DLD of gB and containing an introduced tetracycline cassette) and BAC36.T-KSHV (containing an intact DLD sequence and an introduced tetracycline cassette). Accordingly, BAC36ΔD-KSHV presented significantly lower infection rates in HFF and HMVEC-d cells compared with the comparable infection rates achieved by wild-type BAC36-KSHV and BAC36.T-KSHV. Thus, the present report has delineated a critical role for the DLD of gB in KSHV infection, which may lead to a broader knowledge regarding the sophisticated mechanisms utilized by virus-encoded structural proteins in KSHV entry and infection.

Received 9 April 2014
Accepted 7 May 2014

INTRODUCTION

Since the 1994 discovery of Kaposi's sarcoma-associated herpesvirus (KSHV) in the Chang–Moore laboratory (Chang *et al.*, 1994) 20 years ago, efforts to understand the intricacies of this double-stranded DNA virus have continued. KSHV, also referred to as human herpesvirus-8 (HHV-8), belongs to the gamma-2-herpesvirus subfamily and is the eighth and latest addition to *Herpesviridae* (Russo *et al.*, 1996). KSHV causes a variety of cancers such as Kaposi's sarcoma (KS), primary effusion lymphoma and multicentric Castleman disease (Hamden *et al.*, 2005).

In general, envelope-associated glycoproteins predominantly assist virus in the entry process (Bryan *et al.*, 2005). In this study, our focus is on KSHV glycoprotein B (gB), a lytic structural protein primarily expressed on the envelope of mature virions, but also present on the membrane of cells supporting lytic infection (Akula *et al.*, 2001a). KSHV virus binding and entry has been linked to gB mediated interactions not only with cell surface heparan sulfate (HS) molecules but also to integrins, transmembrane receptor molecules with involvement in processes such as adhesion, motility and endocytosis (Akula *et al.*, 2001a, 2002; Hahn *et al.*, 2009). With KSHV being the first herpesvirus shown to exhibit an interaction with adherent target cell integrins—a preliminary step essential for successful viral infection—it is now known that via its RGD (Arg-Gly-Asp) motif, KSHV gB functionally interacts with a variety of cellular integrins, namely $\alpha 3\beta 1$, $\alpha v\beta 3$ and $\alpha v\beta 5$ (Chakraborty *et al.*, 2012). Unlike the RGD of gB, the disintegrin-like domain (DLD) is a less common integrin recognition motif that was initially identified within the human cytomegalovirus (HCMV) envelope gB (Feire *et al.*, 2010). The DLD in gB was found to bear a striking resemblance to the ADAM (a disintegrin and metalloprotease) disintegrin loop (Feire *et al.*, 2004). Members of the ADAM family are multifunctional proteins that contain a metalloprotease domain and a disintegrin motif that confers RGD-independent

Supplementary material is available with the online version of this paper.

integrin-binding (Feire *et al.*, 2004). It has been observed that KSHV gB possesses a DLD (RX5-7D/ELXXFX5C; 66–85 aa; with a conservative D to E substitution) that is notably conserved among gB homologues of many herpesviruses; specifically beta and gamma herpesviruses (Feire *et al.*, 2010).

Thus, in seeking to delineate a role for the DLD of KSHV gB, we hypothesized the DLD in KSHV gB to play a critical role in the virus infection of cells. Results from our study, using phage display peptide library screening and molecular biology techniques, implicate the ability of the DLD of gB to interact specifically with $\alpha 9\beta 1$ integrins. Utilizing a bacterial artificial chromosome (BAC) system harbouring the KSHV genome (BAC36), we generated two recombinant virus constructs, BAC36ΔD-KSHV (containing alanine point mutations within the DLD sequence of gB and an introduced tetracycline cassette from vector pEX18TC) and BAC36.T-KSHV (containing an intact DLD sequence and the introduced tetracycline cassette from vector pEX18TC) as a means to decipher a potential role for the DLD of KSHV gB in infection of cells.

RESULTS

Expression and purification of gBΔTMΔD

The KSHV-encoded 2106 bp region of the *orf8* gene encoding gBΔTM lacking the transmembrane (TM) and carboxyl domains (Wang *et al.*, 2003) was used to generate a soluble gB lacking a functionally intact DLD, gBΔTMΔD (Fig. 1). This was a crucial step to characterize a role for the DLD of KSHV gB. Coomassie staining of SDS-PAGE gels was conducted to analyse protein purity, and for detection following standard Western blotting protocols (Fig. 2). When purified gBΔTMΔD protein treated with 2-mercaptoethanol (2ME; reducing conditions) was analysed via Coomassie staining, bands of approximately 35–40, 68 and 104 kDa were observed in the lane with gBΔTM (Fig. 2). Impurities such as other contaminating proteins were not detected in either the gBΔTMΔD or the gBΔTM preparations. When gBΔTMΔD and gBΔTM were resolved under non-reducing conditions (−2ME), the 35–40 and 68 kDa bands disappeared while only 104 kDa band and the multiple polypeptides of more than 180 kDa were observed

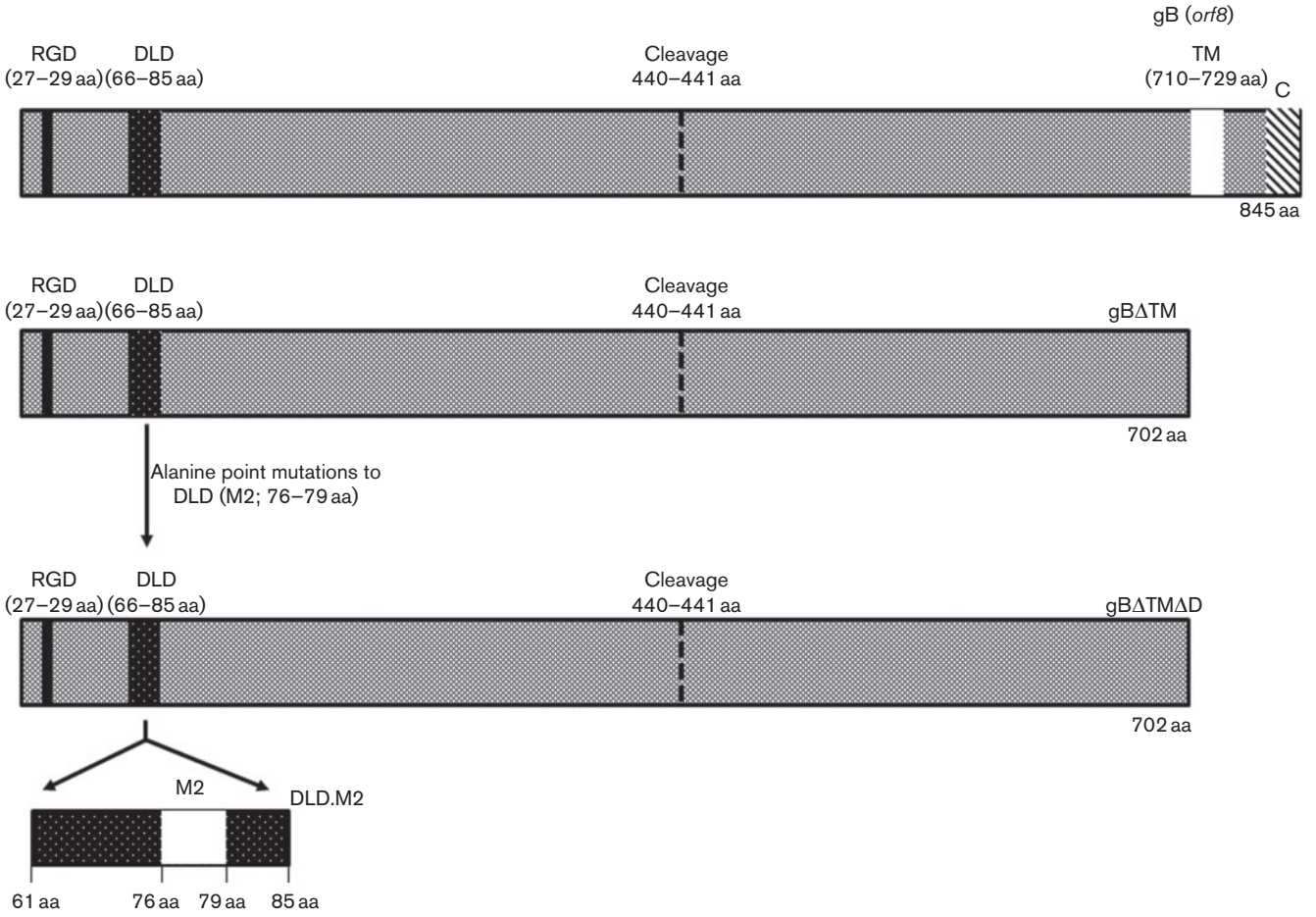

Fig. 1. Generating KSHV gBΔTMΔD. The diagram shows the schematic of gBΔTM and gBΔTMΔD mutant compared with the full-length KSHV gB (*orf8*).

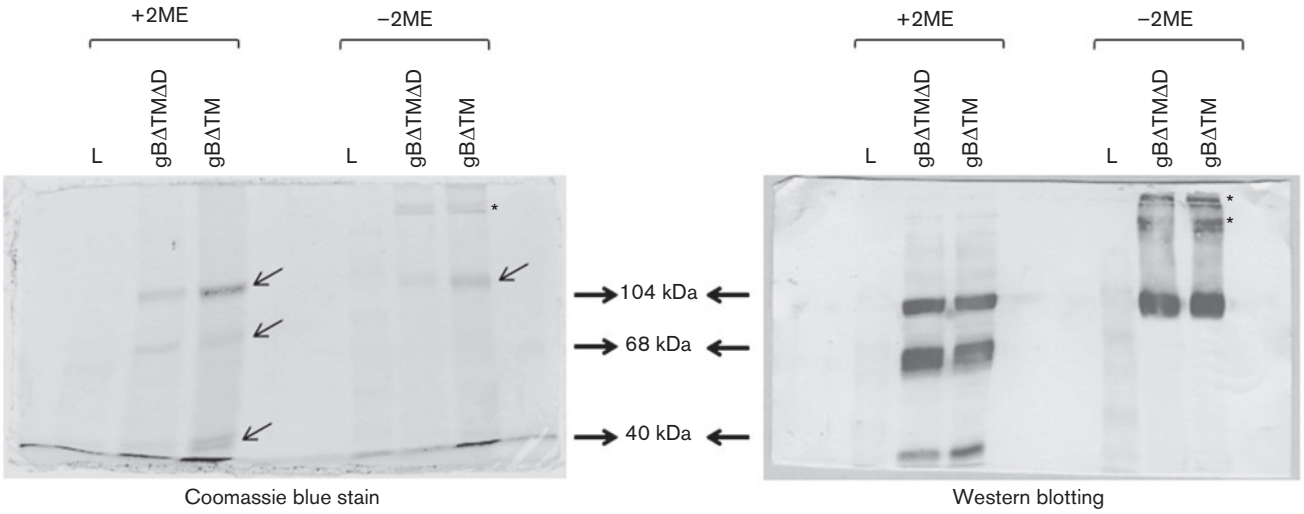

Fig. 2. Expression and purification of gBΔTMΔD in baculovirus expression system. The gBΔTMΔD and gBΔTM were expressed in Sf9 cells and the protein purified from the harvested supernatant using a column containing Ni-NTA agarose beads. Protein purity was analysed by Coomassie staining SDS-PAGE gels and Western blotting procedures using rabbit polyclonal antibodies to full-length gB. Experiments were performed under reducing (+2ME) and non-reducing conditions (−2ME). Under non-reducing conditions, an upward shift in the migration pattern of both the proteins is indicated by asterisks. Arrows denote the bands corresponding to recombinant gB.

(Fig. 2). The migration pattern of gBΔTMΔD was comparable to what was observed when gBΔTM was resolved in earlier studies (Dyson *et al.*, 2010; Wang *et al.*, 2003). The specificity of the gB proteins was confirmed by performing Western blotting experiments (Fig. 2). This implies that gBΔTMΔD, like gBΔTM, expressed in *Spodoptera frugiperda* (Sf9) ovarian cells can form disulfide-linked dimers or multimers under non-reducing conditions. These results suggest that the alanine point mutations introduced in the DLD sequence of gB did not significantly change the molecular mass or the migration pattern of the protein on gels compared with the wild-type (gBΔTM).

Phage display (PhD) peptide library identifies integrin α9 as a potential receptor for DLD in gB

The PhD phage display library was used to identify novel ligands for the DLD in gB. Three random peptide libraries, a linear (X)7, a cyclic Cys (X)7 Cys and a linear (X)12 were screened against the gB DLD peptide. The single most common peptide (based on the increased frequency; 20 out of 30) possessed a **PKA**(P)**DGR**(H)**V**(L) sequence (Table 1). Interestingly, the major conserved sequence among the peptides identified had a conserved sequence of PKADGRV (9 out of 30).

We tested the ability of the phage carrying peptides L3 (PKADGRV), F1 (DCK**PKPDGRL**RD) and F5 (PKADGHV) to bind gBΔTM immobilized on 96-well plates. It was determined that the phage carrying peptides L3, F1 and F5 bound gBΔTM more efficiently than BSA and gBΔTMΔD (Fig. 3a). However, the phage encoding peptide PKADGRV (peptide L3) bound more efficiently than the other peptides (F1 and F5). The binding of the phage encoding L3 peptide to gBΔTM could be significantly blocked by including 1 mM of synthetic peptide PKADGRV during the incubation step compared with using scrambled peptide (Fig. 3b). The effect of PKADGRV peptide was measured against the known positive control, gBDLD peptide (Fig. 3b). A BLAST protein search of this sequence identified α9 integrin (*Homo sapiens*; NCBI Ref Seq: NM_002207.2) to possess such a motif (133–139 aa). This was an interesting finding, because at the beginning of the study we had predicted a non-RGD binding integrin (Yokosaki *et al.*, 1994) as a probable receptor capable of binding the DLD of gB.

Table 1. Amino acid sequences of the phage-displayed peptides isolated by screening against DLD in gB

Name	Sequence	Frequency
L3	**P K A D G R V**	9
L5	M T A E N I R	1
F1	D C K **P K** P **D G R** L R D	6
F3	Q A M S D K F R C G W A	2
F5	**P K A D G** H **V**	5
F9	C N H P L E C	1
S6	P Y H D Q I A	1
S8	L R **P** R **A D G** P T E F W	2
S9	S W A D T T I Q Y V V L	1
S4	R F I Y P E D P F I E C	1

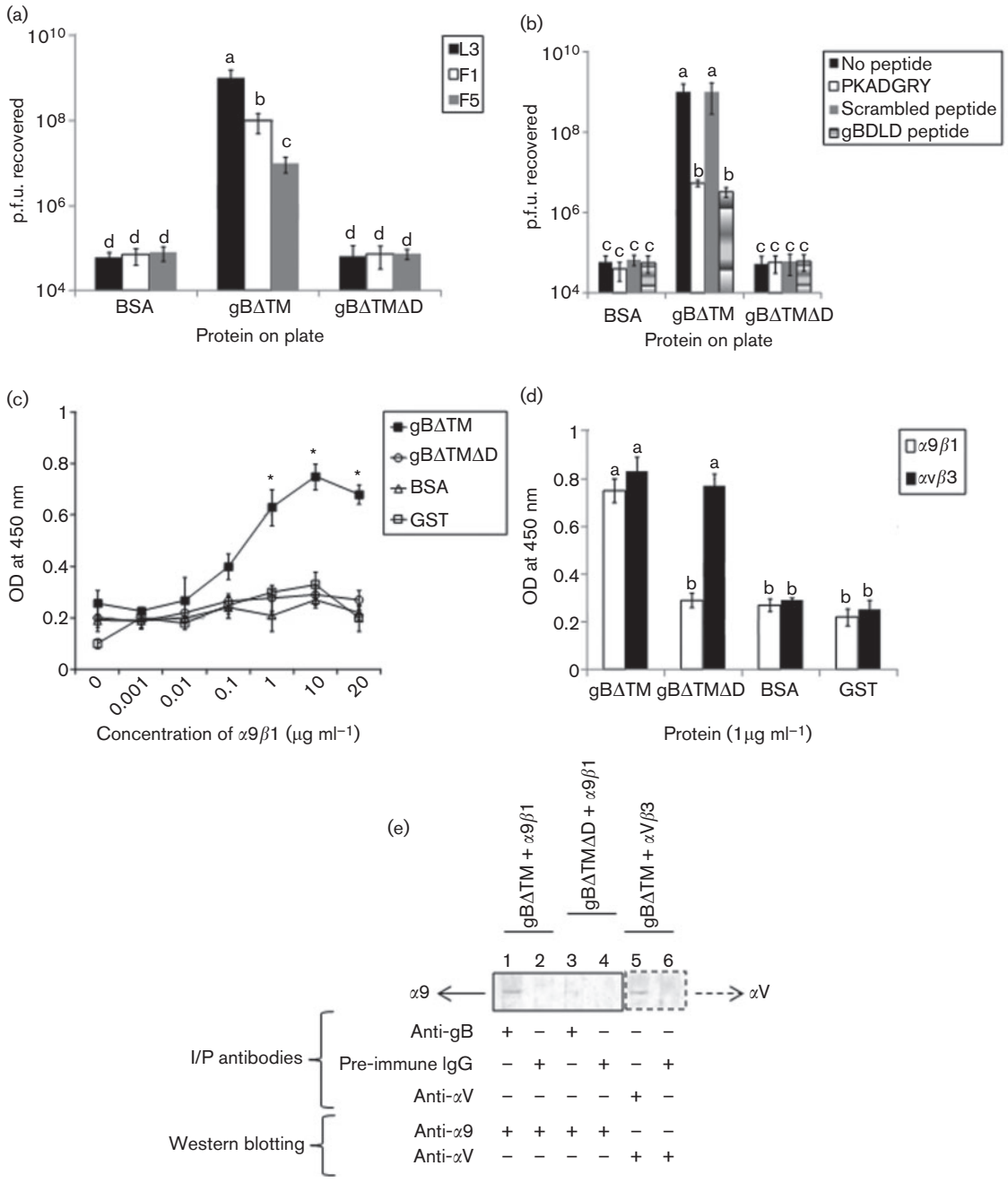

Fig. 3. Phage encoding peptide PKADGRV bound gBΔTM efficiently. (a) p.f.u. recovered when 10^{11} p.f.u. of phage carrying peptides L3, F1 and F5 were screened against immobilized gBΔTM, gBΔTMΔD, or BSA (negative control) proteins on microplates. (b) p.f.u. recovered when 10^{11} p.f.u. of phage carrying peptide L3 was screened against immobilized gBΔTM, gBΔTMΔD, or BSA on microplates in the absence or presence of 1 mM solution of PKADGRV, gBDLD peptide, or scrambled peptide. Finally, ELISA was performed to determine the interactions between (c) $\alpha 9\beta 1$ or $\alpha v\beta 3$ (d) with immobilized gBΔTM, gBΔTMΔD, BSA, or GST. Each point denotes the average ± SD (error bars) of three experiments. Columns with different alphabets and asterisks on the data points denote the value to be statistically significant ($p<0.05$) by least significant difference (LSD). (e) Immunoprecipitation experiments to demonstrate gB interactions with $\alpha 9\beta 1$. Recombinant gBΔTM (lane 1) compared with gBΔTMΔD (lane 3) specifically bound α9. As a positive control, gB interactions with $\alpha V\beta 3$ was tested.

Plate-based binding assays demonstrate the DLD of KSHV gB to bind α9β1

The integrin α9 commonly forms a heterodimer with β1 integrin subunit, α9β1 (Young *et al.*, 2001). Upon identifying the α9 integrin as a plausible receptor for gB, we used various modified ELISAs to test the ability of soluble KSHV gB to bind α9β1. The binding of α9β1 to gBΔTM was monitored using polyclonal antibodies to α9β1 (H-198). ELISA studies identified α9β1 to bind specifically 1 μg ml^{-1} of gBΔTM in a dose-dependent manner (Fig. 3c) compared with gBΔTMΔD and non-specific controls, BSA or GST. Similar data were observed when monoclonal antibodies to α9β1 (clone #560201) were used in the ELISA (data not shown). Interestingly, ELISA studies demonstrated an RGD binding integrin αvβ3, to bind gBΔTM and gBΔTMΔD to comparable extent (Fig. 3d), demonstrating a functional RGD motif in both the soluble forms of the gB tested. Based on these results, 1 μg ml^{-1} of both gBΔTM and α9β1 were used in all our other experiments described below. An immunoprecipitation experiment was done to authenticate further the results from ELISA-based assays. Herein, the α9 subunit was found to bind specifically gBΔTM (Fig. 3e, lane 1) and not the gBΔTM lacking a functional DLD (Fig. 3e, lane 3).

To confirm the specificity of the KSHV-encoded gB:α9β1 binding, we attempted to neutralize this interaction by conducting competitive ELISAs. In this case, different concentrations of various ligands or antibodies known to interact with gB, the DLD motif specifically, or α9β1 were used. KSHV gB is known to interact with HS via a charge based interaction (Bryan *et al.*, 2005). HS, chondroitin sulfate-A or -B (CSA, CSB; control glycosaminoglycans) had little effect on the gB:α9β1 interactions, as binding between gBΔTM and α9β1 still occurred (Fig. 4a).

KSHV gB interacts with a variety of integrins via its RGD domain. In order to determine if gB interactions via the RGD domain altered its ability to bind α9β1, competitive ELISA using G**RGD**SP and KQAGDV (an irrelevant peptide) was performed. The results confirmed that increasing concentrations of RGD peptides did not alter the ability of α9β1 to bind gBΔTM (Fig. 4b). Interestingly, the RGD peptide significantly blocked the ability of αvβ3 to bind gBΔTM (Fig. S1, available in the online Supplementary Material).

VEGF and tenascin C are common known ligands for integrin α9β1 (Andrews *et al.*, 2009; Vlahakis *et al.*, 2005). Our data suggest that increasing concentrations of VEGF and laminin did not alter the binding of α9β1 to gBΔTM

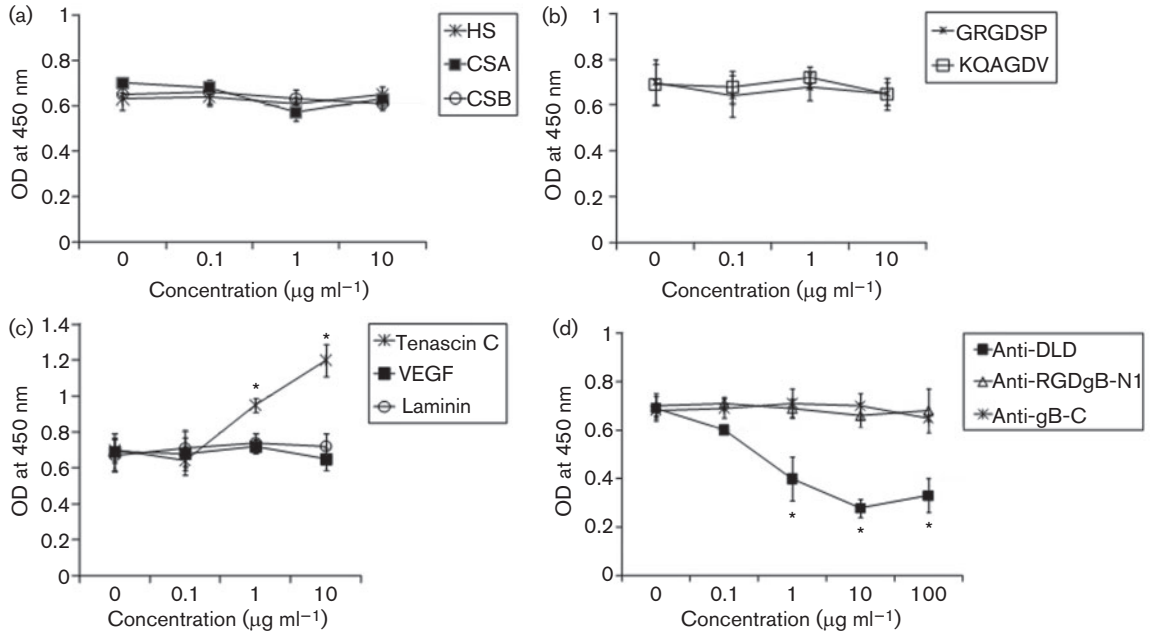

Fig. 4. gB:α9β1 interactions characterized by performing competitive ELISA. ELISA was performed using a constant concentration of 1 μg ml^{-1} for both α9β1 and bound gBΔTM. (a) Increasing concentrations of HS in PBS (or CSA and CSB) were incubated in gBΔTM-coated wells prior to incubating with α9β1 and performing the ELISA. (b) Increasing concentrations of GRGDSP and KQAGDV (an unrelated peptide). Tenascin C, VEGF and laminin (c) were incubated with α9β1 for 30 min at room temperature (in an additional step) prior to their addition into gBΔTM-coated wells and performing ELISA. (d) gBΔTM-coated plates were incubated with anti-DLD or additional non-specific antibodies prior to incubation with α9β1 and performing ELISA. The results were read at 450 nm (OD 450). Data are the means ± SD (error bars) of three experiments. Asterisks denote statistical significance ($P<0.05$) by LSD.

(Fig. 4c). Tenascin C, on the other hand, was shown to enhance the gB:α9β1 binding interaction (Fig. 4c).

Finally, to confirm whether gB:α9β1 binding is dependent on the DLD of gB, we conducted competitive ELISAs using rabbit antibodies to DLD of gB (anti-DLD). Here, results show that there was a significant inhibition in the ability of α9β1 to interact with gBΔTM when the gBΔTM-coated wells were incubated with anti-DLD prior to performing ELISA (Fig. 4d). Incubating gBΔTM-coated wells with anti-RGDgB-N1 or anti-gB-C (non-specific antibodies) did not alter the ability of α9β1 to bind gBΔTM (Fig. 4d). In addition, the anti-RGDgB-N1 antibodies blocked αvβ3 binding to gBΔTM (Fig. S1), suggesting the specificity of antibodies to DLD of gB to block gB:α9β1 interactions. ELISA yielded identical results when performed at room temperature or at 37 °C (data not shown).

Inhibiting interactions between α9β1 and the DLD of gB lowers KSHV infection

To confirm a critical role for the DLD:α9β1 interactions in KSHV infection we utilized the recombinant KSHV that expressed green fluorescent protein (GFP) referred to as rKSHV.152 (Akula *et al.*, 2001b; Grange *et al.*, 2012; Vieira *et al.*, 2001) and three different cell types known to support KSHV infection of cells. They were human foreskin fibroblasts (HFFs), human embryonic kidney 293 epithelial cells (293 cells) and human microvascular endothelial (HMVEC-d) cells. First, we determined if these cells actually did express α9. PCR results demonstrated HFF and HMVEC-d cells to express α9 compared with 293 cells (Fig. 5a). Both HFF and HMVEC-d cells expressed α9 on their cell surface as monitored by flow cytometry (Fig. 5b) and immunofluorescence assay (Fig. S2). Interestingly, all of the above cells (including the commonly used B-cell line, BCBL-1) express the β1 integrin subunit (Akula *et al.*, 2002). Next, we conducted rKSHV.152 infection-based studies in the above cells using appropriate antibodies (Fig. 5c). Expression of GFP by cells was considered as positive for rKSHV.152 infection (Akula *et al.*, 2001b). This expression of GFP was monitored using a fluorescent microscope. The numbers of GFP positive cells at 72 h post-infection (p.i.) in 293, HFF and HMVEC-d cells that were untreated with antibodies were 260, 50 and 105, respectively. Antibodies to α5 and a pre-immune IgG did not significantly alter rKSHV.152 infection of cells (Fig. 5c). Soluble heparin was used as a known inhibitor of KSHV binding and infection of all the target cells. Antibodies to β1 and αV integrins significantly inhibited rKSHV.152 infection of cells in HFF and HMVEC-d cells compared with infection in 293 cells (Fig. 5c). Infection of HFF by rKSHV.152 was significantly lowered by antibodies to α9. We observed only a modest inhibition of rKSHV.152 infection by antibodies to α9 in HMVEC-d cells. A dose-dependent effect of the antibodies to α9 on rKSHV.152 infection is shown in Fig. S3. These results suggest an involvement of α9β1 integrin in the KSHV infectious process of HFF cells and to a modest extent in HMVEC-d cells. To further authenticate the above results, we tested the effect of incubating rKSHV.152 with the soluble α9β1 integrin prior to infecting the target cells. A dose-dependent inhibition of KSHV infection of cells was observed when rKSHV.152 was incubated with soluble α9β1 compared with α5β1 (Fig. S4) prior to infection of HFF and HMVEC-d compared with 293 cells (Fig. 5d). The soluble α9β1 used in this study was in a lyophilized form that was resuspended in sterile PBS. Finally, we tested the effect of incubating KSHV with rabbit antibodies developed against the DLD peptide sequence of gB prior to infection of cells. Our results indicated incubating KSHV with antibodies to DLD or RGD of gB lowered KSHV infection of HFF and HMVEC-d cells compared with 293 cells (Fig. 5e). Overall, these results implicate a key role for α9β1:DLD interactions in KSHV infection of HFF and HMVEC-d cells (with minor differences between cell types as noted in the Discussion).

DLD of gB is critical to KSHV infection of cells

We hypothesized that knocking down a functional DLD of gB in KSHV will result in a decrease in virus infection of cells. To test this hypothesis, we developed a recombinant virus that lacked a functional DLD in KSHV gB (BAC36ΔD-KSHV). As a control to the BAC36ΔD-KSHV, we also generated BAC36.T-KSHV that had an uninterrupted and functional gB, but with a tetracycline cassette (as in BAC36ΔD) introduced in the intron region between the *orf8* and *orf9*. In brief, employing overlap PCR (Fig. 6a, b), a series of cloning experimentations and then recombination rendered BAC36ΔD and BAC36.T clones, respectively (Fig. 6c). Prior to transformation via electroporation and tetracycline selection stages, the correct orientation of the inserted tetracycline cassette in *orf8ΔDLD.Tet^r/TOPO* and *orfΔ7.8.Δ9.Tet^r/TOPO* positive clones was confirmed by restriction enzyme digestion using *Bam*HI and *Nhe*I; clone #3.2 and clone #7.2, denoting *orf8ΔDLD.Tet^r/TOPO* and *orfΔ7.8.Δ9.Tet^r/TOPO* respectively, contain the correctly oriented cassette and were subsequently used in the generation of BAC36ΔD and BAC36.T clones (Fig. S5A). These clones were further compared with the BAC36 wild-type and confirmed by performing a variety of PCRs. First, PCR amplified tetracycline gene in BAC36ΔD and BAC36.T compared with the BAC36 (Fig. S5B). All of the recombinant viral genomes contained the *orf8* gene as determined by PCR (Fig. S5B). Second, we confirmed that targets 1 and 2, representing a portion of *orf7*, the complete sequence of *orf8* and the N-terminal sequence of *orf9* from the original BAC36 genome (Fig. S5B), were contained in BAC36ΔD and BAC36.T (Fig. S5C). Third, we amplified *orf8* from the BAC36, BAC36ΔD, BAC36.T genomes using T1(F) and T2(R) primers. As predicted, we amplified a 4005 bp DNA fragment in the BAC36 genome, while amplifying a product of size 5698 bp from both BAC36ΔD and BAC36.T (Fig. S5D). The above results were authenticated by sequencing using appropriate primers to confirm the specific mutations in the *orf8* gene contained within the BAC36ΔD (Fig. S5E).

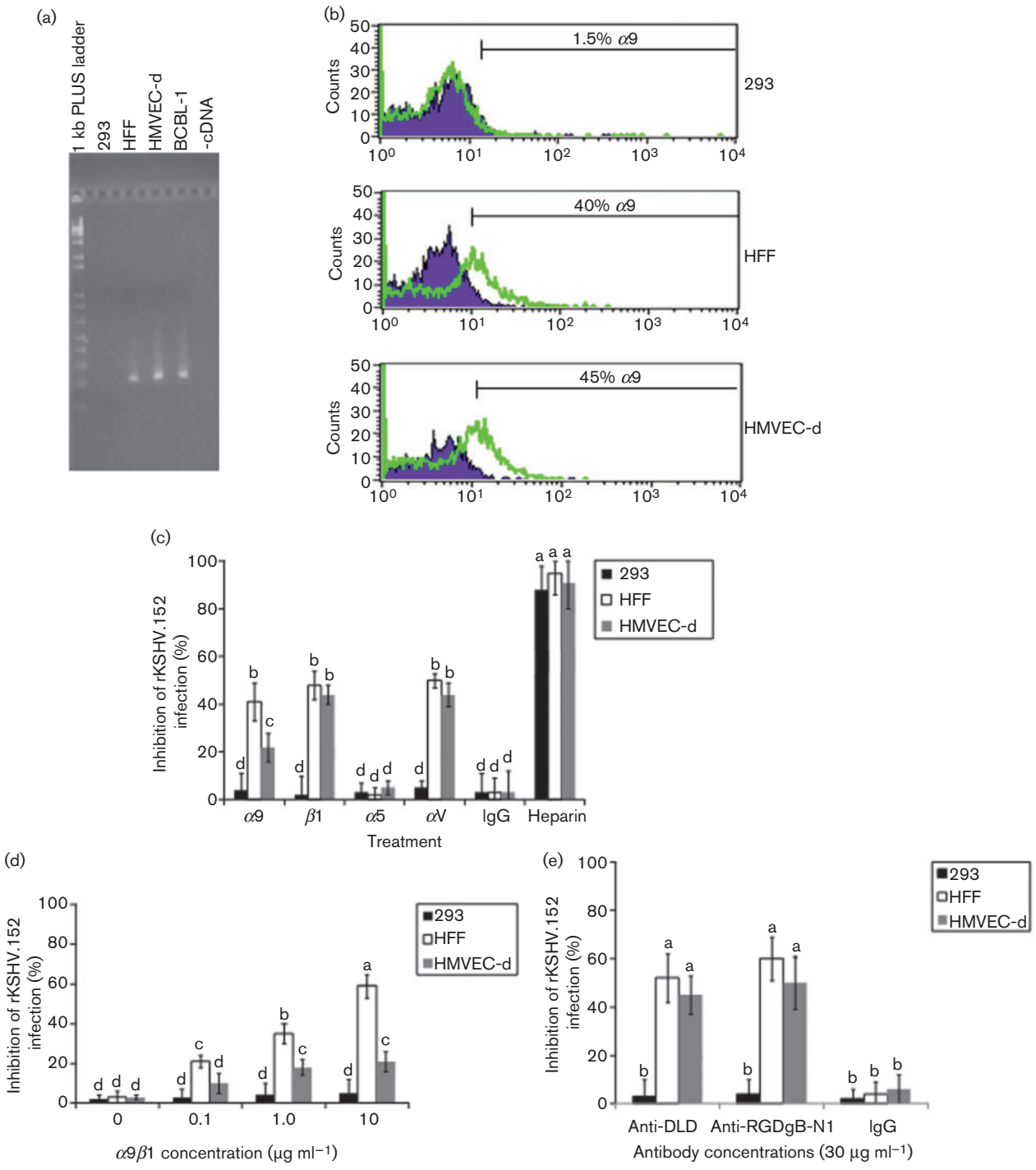

Fig. 5. Role of integrin α9β1 in wild-type KSHV infection. (a) HFF, HMVEC-d and BCBL-1 cells express α9. cDNA synthesized from target cells was subjected to PCR analysis to amplify a α9 PCR product (α9: ~190 bp) that was resolved in a 2.1 % agarose gel. (b) Flow cytometry analysis of the surface expression of α9 integrin subunit in 293, HFF and HMVEC-d cells was performed following staining with Integrin α9 (H-198) rabbit polyclonal antibody and subsequent incubation with goat anti-rabbit FITC. The average percentage of cells positive for the α9 expression from three independent experiments is shown above the marker. Representative histogram plots show interactions with pre-immune IgG (purple plot) and anti-α9, (green outline) for each cell type. (c–e) Inhibition of rKSHV.152 infection by 20 μg ml^{-1} of antibodies to integrins (c), soluble integrin (d) and 30 μg ml^{-1} of anti-DLD antibodies (e) is shown. In the above experiments (panels c–e), infection was monitored at 72 h p.i. by recording the total number of cells expressing GFP under a fluorescent microscope. Data are presented as percentage of inhibition of the virus infectivity obtained when the cells were pre-incubated with Dulbecco's modified eagle medium as a control. Data are the means ± SD (error bars) of three experiments. Letters above columns indicate statistical significance ($P<0.05$) by LSD.

We then tested the infection rates of the above different recombinant viruses generated in the lab. First, we analysed cell surface expression of gB in BAC36-KSHV and BAC36ΔD-KSHV infected cells by FACS. This is vital, as the results demonstrated that cell membrane expression of gB in 12-O-tetradecanoyl-phorbol-13-acetate (TPA)-induced 293 cells infected with BAC36-KSHV and BAC36ΔD-KSHV was comparable (Fig. 7a). Next, we monitored infection of BAC36-KSHV, BAC36ΔD-KSHV, BAC36.T-KSHV in 293, HFF and HMEVC-d cells as per standard procedures. Our results indicated a sharp decline in the BAC36ΔD-KSHV infection of HFF and HMVEC-d cells compared with BAC36-KSHV and BAC36.T-KSHV, respectively (Fig. 7b). Interestingly, BAC36ΔD-KSHV infection of 293 cells was not altered compared with BAC36-KSHV and BAC36.T-KSHV (Fig. 7b). The numbers of GFP positive cells at 72 h p.i. of BAC36-KSHV in 293, HFF and HMVEC-d cells were 116, 28 and 57, respectively. Taken together, our results implicate a critical role for DLD of gB in KSHV infection of HFF and HMVEC-d cells.

DISCUSSION

In addition to the most common integrin recognition motif, RGD (Akula *et al.*, 2002; Garrigues *et al.*, 2008), KSHV gB also possesses DLD juxtaposed in the extracellular amino terminal coil region that also has potential integrin-binding capabilities (Feire *et al.*, 2004). In fact, it was the analysis of the related domains of snake venom metalloproteases (SVMPs) that sparked the assumption that other varieties of DLDs, such as in ADAMs, would also be involved in integrin-mediated interactions (Lu *et al.*, 2010; Wolfsberg *et al.*, 1995).

The DLD of KSHV gB (66–85 aa) corresponds to 49–68 aa residues within the EBV gB. EBV is a human herpesvirus closely associated to KSHV, and both are classified as gamma herpesviruses. Earlier, the ectodomain (23–685 aa out of a full 1–875 aa length) of EBV gB was crystallized (Backovic *et al.*, 2009). It was determined that the major portion (52–68 aa) of the electron-dense DLD of EBV gB is contained within the domain III region, which is exposed and actually wraps around the helices to form a left-handed twist. Based on these findings, we predict the DLD of KSHV gB also to be an exposed ectodomain available for interactions with host cell receptor molecules. Outside HCMV, the role of DLD in virus entry has been minimally explored. Thus, this study has sought to unearth the role of DLD of gB in KSHV infection.

Instead of employing antibody-based assays, we utilized phage display peptide library screening to ascertain the putative receptor for the DLD of KSHV gB. We determined the DLD of gB to interact with the host cell receptor molecule, integrin α9, by panning random libraries of phage displayed peptides against the gBDLD peptide fragment (Table 1; Fig. 3a, b). The results from screening the phage display peptide libraries were further authenticated by performing plate-based binding assays (ELISAs) and immunoprecipitation experiments using both gBΔTM and gBΔTMΔD (Fig. 3c, d).

The subunit α9 has been widely shown to combine with β1 to form a single heterodimer (Young *et al.*, 2001) with non-RGD binding capabilities (Yokosaki *et al.*, 1994). For this study, insight regarding specificity of KSHV gB:α9β1 interactions was provided from results of several competitive ELISAs. HS (Fig. 4a), a target cell membrane molecule whose interaction with KSHV is mediated in part by envelope gB (Bryan *et al.*, 2005), VEGF, a known ligand for α9β1 (Vlahakis *et al.*, 2005), or laminin, an extracellular matrix protein (Fig. 4c), did not block the gB:α9β1 interactions. Another known ligand for α9β1, tenascin C (Andrews *et al.*, 2009), also failed to neutralize the gB:α9β1 interaction (Fig. 4c). In the case of tenascin C, however, enhanced binding was observed between gBΔTM and α9β1 in what we believe to be a result of an allosteric interaction (Fig. 4c), as suggested by an earlier report (Laskowski *et al.*, 2009). Tenascin C is an extracellular matrix (ECM) molecule that is frequently expressed at elevated levels in solid tumours and is said to have a role in cancer formation (Orend & Chiquet-Ehrismann, 2006). Further studies will focus on appreciating gB:α9 interactions with respect to tenascin C expression.

Likewise, competitive ELISAs also confirmed the ability of KSHV gB to interact with integrin α9β1 independent of its RGD domain (Fig. 4b). Our findings are reminiscent of results produced by Eto *et al.* (2002) who found that mutating the RGD motif of the aforementioned ADAM-15, had no effect on the binding of α9β1 to the protein's disintegrin domain. Moreover, when using an antibody directed against the DLD in gB, competitive ELISA data showed a substantial downregulation of the gB:α9β1 interactions, suggesting the specificity of this antibody (Fig. 4d). These results imply that the avid binding between gB and α9β1 is in fact dependent on the DLD of KSHV gB (Fig. 4d).

In an effort to extrapolate plate-based assays to viral infection, we attempted to test the role of integrin α9β1 in wild-type KSHV infection of different cells (Fig. 5). HFF and HMVEC-d cells express α9β1, but 293 cells do not. KSHV infection of 293 cells was not altered by antibodies to α9, β1 subunits, DLD target sequence, and soluble α9β1 (Fig. 5c, e). In HFF cells, antibodies to α9, β1 subunits, DLD target sequence, and soluble α9β1, significantly lowered KSHV infection (Fig. 5c e). In HMVEC-d cells, there was a significant decrease in KSHV infection of cells due to antibodies against β1 subunit and the DLD target sequence, with only a modest decrease in infection noticed due to antibodies against α9 and soluble α9β1 (Fig. 5c, e). Taken together, from the above results we conclude the following. (i) The α9β1:DLD of gB interactions may be required for an efficient KSHV infection of HFF cells. The DLD interactions may well play a supportive role to the RGD interactions with integrin(s) (Chandran, 2010; Veettil *et al.*, 2008) in promoting virus entry. (ii) There may be another non-RGD

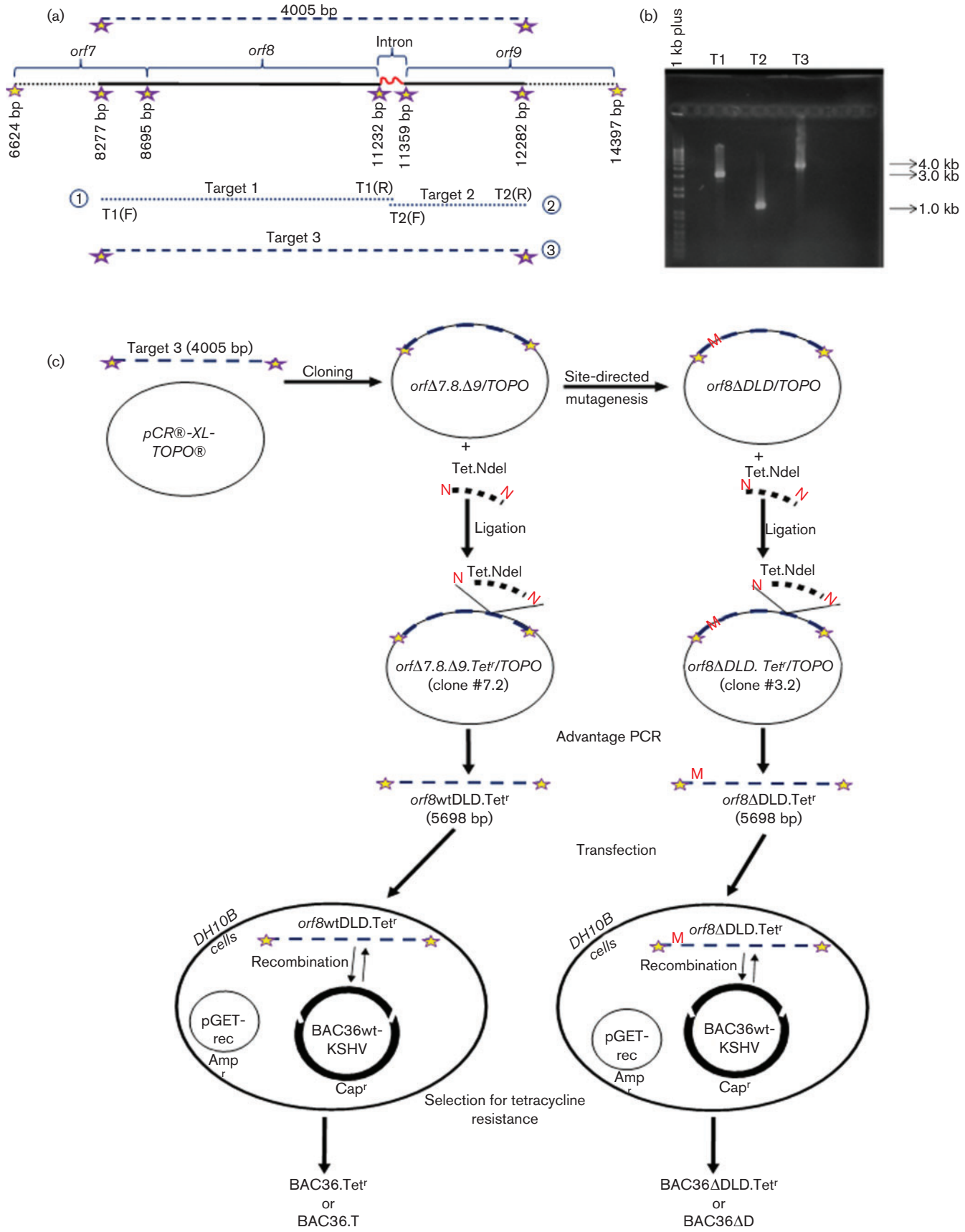

Fig. 6. Legend on following page.

Fig. 6. Architecture and generation of recombinant BAC36ΔD. (a) Diagram of how the target 3 PCR product was obtained. (b) DNA agarose gel electrophoresis of purified targets to confirm predicted fragment sizes. Elution-purified target 1 (T1; 2967 bp), target 2 (T2; 1055 bp) and gel-purified target 3 (T3; 4005 bp) were resolved in 1 % agarose gels and stained by ethidium bromide. Bands of expected sizes were rendered. (c) Schematic depiction of the molecular biology procedures involved in the construction of BAC36ΔD and BAC36.T clones. A detailed description concerning the construction of the clones is provided in the online Supplementary Material.

binding integrin receptor(s) with which DLD of gB interacts in promoting virus infection of HMVEC-d cells. (iii) KSHV utilizes diverse mechanisms to enter a variety of target cells.

The use of soluble integrins and antibodies to define a crucial role for a receptor molecule is not without its limitations, primarily depending upon the purity, function and concentrations of the recombinant proteins or the antibodies. Hence, we generated BAC36ΔD-KSHV (KSHV lacking the functional DLD) to appreciate more completely the physiological role for DLD in virus infection of cells (Fig. 7). Recently, upon sequencing the KSHV-BAC36 genome in its entirety, Yakushko *et al.* (2011) discerned a 9 kb long unique region (LUR) fragment duplication in the terminal repeat region of several viral stocks acquired by laboratories. However, we assume this did not complicate our generation of BAC36ΔD and BAC36.T, as our modifications to BAC36 did not involve mutagenesis to viral genes located within the potential LUR duplication. Here, the infection of BAC36ΔD-KSHV was compared with BAC36-KSHV wild-type and BAC36.T-KSHV in 293, HFF and HMVEC-d cells (Fig. 7). The results indicated comparable infection rates for BAC36-KSHV and BAC36.T-KSHV in all tested cell types (Fig. 7). However, the infection rates for virus lacking an intact DLD of gB were significantly lower in HFF and HMVEC-d cells compared with 293 cells (Fig. 7), which provides evidence that the DLD of KSHV gB and its interaction with $\alpha 9\beta 1$ has a substantially important role in regulating virus infection. Our results also confirm KSHV to utilize a mechanism of entry into 293 cells that is independent of $\alpha 9\beta 1$. Earlier studies also determined KSHV infection of 293 cells to be via binding heparin sulfate, but independent of RGD integrins (Inoue *et al.*, 2003). At this stage, we can only hypothesize that such an efficient internalization of KSHV by 293 cells occurs as a result of a dynamic and biologically active cell membrane of a transformed cell line compared with primary cells such as HFF and HMVEC-d cells.

Multiple studies have determined that interactions of the gB RGD with $\alpha 3\beta 1$, $\alpha V\beta 3$ and $\alpha V\beta 5$ are necessary for KSHV entry (Chandran, 2010; Veettil *et al.*, 2008). KSHV has also been shown to use DC-SIGN and the 12-transmembrane glutamate/cysteine exchange transporter protein xCT as receptor molecules in dendritic cells, macrophages and activated B cells (Rappocciolo *et al.*, 2008, 2006; Zhang & Gao, 2012). Recent studies by Hahn *et al.* (2012) deciphered a key role for gH/gL interactions with EphA2, a tyrosine kinase, in promoting virus entry. Like other viruses, KSHV has evolved to utilize different combinations of host cell

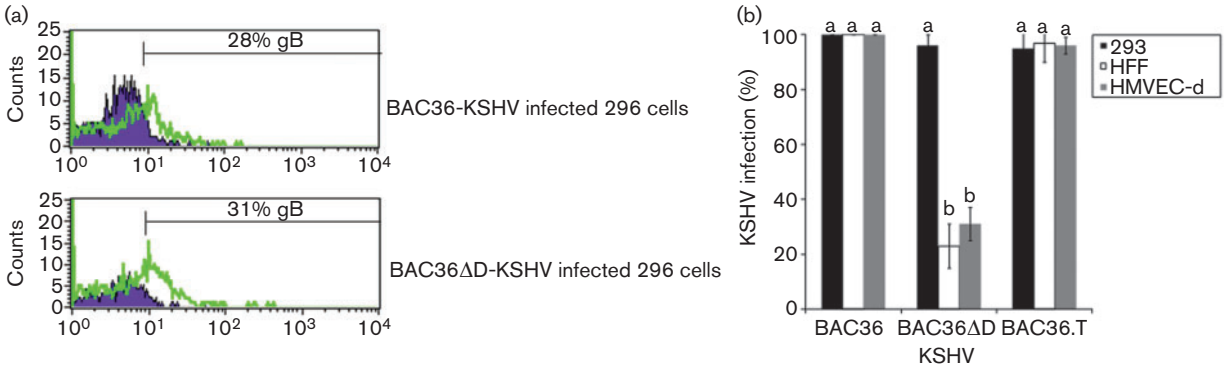

Fig. 7. DLD of gB is critical for KSHV infection. (a) Monolayers of 293 cells were infected with 0.1 m.o.i. of BAC36-KSHV or BAC36ΔD-KSHV. At 48 h p.i., the cells were treated with TPA for 72 h. These cells were analysed for the surface expression of gB in 293 cells by staining with pre-immune IgG (solid purple) or rabbit polyclonal anti-gB antibody (green outline) followed by incubation with goat anti-rabbit FITC before examining by FACS. The average percentage of cells positive for the surface expression of gB from three independent experiments is shown above the marker. A representative histogram plot for each cell type is depicted. (b) Monolayers of 70–80 % confluent 293, HFF and HMVEC-d cells were infected with BAC36-KSHV, BAC36ΔD-KSHV, or BAC36.T-KSHV. At 72 h p.i., the total number of cells expressing GFP was counted under a fluorescent microscope. The percentage of target cells infected with BAC36-KSHV is shown. Data shown are the means ± SD (error bars) of three experiments. Letters above columns indicate statistical significance ($P<0.05$) by LSD.

receptor molecules to infect target cells, and integrin $\alpha9\beta1$ could well be the latest addition to KSHV's arsenal of host cell receptor molecules utilized for entry.

Though these findings delineate a critical role for the lesser studied integrin-binding domain (DLD) of gB in KSHV infection, this study has also led to the opening up of other questions that await our further research. Importantly, we seek clarity regarding the manner by which the $\alpha9\beta1$:DLD-induced cellular signalling alters initial stages of virus infection (i.e. virus binding, initial target cell entry, escape to the endosome, or eventual nuclear transport). Additionally, we seek to understand how reactions involving DLD of gB and integrins support RGD-dependent interactions critical to virus entry. Do these seemingly mutually exclusive integrin-binding motifs within gB somehow work in concert to regulate virus infection? Moreover, ongoing studies will also monitor the possibility of integrin heterodimer $\alpha9\beta7$ interaction with DLD of KSHV to regulate virus infection, much like the ability of ADAM-2 in RPMI 8866 cells (which express little or no $\beta1$) to interact with $\alpha9\beta7$ (Desiderio *et al.*, 2010). All further studies in this area will strive for a better understanding of the intricacies involved in the role of, and mechanisms utilized by, glycoproteins in KSHV entry and infection.

METHODS

Cells. HFF cells, 293 cells, HMVEC-ds (CC-2543; Clonetics) and Sf9 ovarian cells were propagated as per standard laboratory protocols (Akula *et al.*, 2005).

Antibodies. An antibody to DLD peptide sequence of gB (anti-DLD) was generated in rabbits by Pi-Proteomics and used in ELISAs performed in this study. Rabbit antibodies to the RGD-containing sequence of gB (anti-RGDgB-N1) and a peptide sequence from the C-terminal domain in gB (anti-gB-C) were also used. Antibodies to full-length gB, RGDgB-N1 and gB-C have been described in earlier studies (Akula *et al.*, 2002). Human $\alpha9$ (H-198) rabbit polyclonal antibodies (Santa Cruz Biotechnology), $\alpha9$ monoclonal mouse IgG clone #560201 (R & D Systems), αV monoclonal mouse IgG (clone P3G8; Millipore), $\alpha5$ monoclonal mouse IgG (clone P1D6; Millipore) and $\beta1$ monoclonal mouse IgG (clone 6S6; Millipore), were also used in this study.

Proteins and peptides. See the online Supplementary Material for a full description.

Cloning and expression of recombinant gBΔTMΔDLD.H. His-tagged, recombinant and soluble KSHV gBΔTM and gBΔTM lacking the DLD (gBΔTMΔD) were expressed and purified from Sf9 cells as per earlier studies (Dyson *et al.*, 2010; Wang *et al.*, 2003).

Western blotting. Equal concentrations of soluble gB proteins (25 μg) were resolved on SDS-PAGE gels prior to being transferred to a PVDF membrane that was probed using rabbit polyclonal antibodies to gB and appropriate secondary antibodies as per earlier studies (Dyson *et al.*, 2012).

PCR. PCR assays were conducted using synthesized cDNA and specific primers (Table 2). PCR amplifications were performed using Platinum *Taq* DNA Polymerase, High Fidelity (Life Technologies) and/or Advantage cDNA PCR kit (BD Biosciences Clontech) at appropriate annealing temperatures and extension times. Amplified products were separated on agarose gels, and expression was monitored.

Screening phage display peptide libraries to determine a novel receptor for gB. A detailed protocol is provided in the online Supplementary Material.

ELISA. To characterize the binding interactions between soluble gB and integrin $\alpha9$, ELISA was performed as per standard protocols. A detailed protocol is provided in the online Supplementary Material.

Immunoprecipitation. Soluble integrins (1 μg ml^{-1}) were incubated with different forms of 1 μg ml^{-1} of recombinant gB for 2 h at 4 °C.

Table 2. List of primers

Primer	Sequence
α9.FW2.Q.F	GATGAGTGGATGGGGGTGAG
α9.FWQ.R	CCGTGTTCCTCTCCGTACTT
DLD-M2 (F)	TCGATCACCGGGGAG**GCGGCGGCGGCG**AACCTGGAGCAGACG
DLD-M2 (R)	CGTCTGCTCCAGGTT**CGCCGCCGCCGC**CTCCCCGGTGATCGA
pHHV8gB (F)	AGTGAGGATCCACAATGACTCCCAGG
ORF8.HIS (R)	TCCGAATTCTCAATGATGATGATGATGGCCACCCAGGTCCGCCACTATCTC
ORF8.RD (F)	ATGACTCCCAGGTCTAGATT
ORF8.D (F)	AAGCATCTGGTCCTAAGAGT
ORF8.RD (R)	TCGTTGGCCACAAAGTGGAA
ORF50P8.ChIP.OD (F)	CTACCGGCGACTCATTAAGC
ORF50P8.ChIP.OD (R)	GTGGCTGCCTGGACAGTATT
T1 (F)	GTGACGCTGGCTCAGTGCTTCGAGGCTGCGGGCATGCTT
T1 (R)	TCGAATCATATGTCACTCCCCCGTTTCCGGACTGATGTC
T2 (F)	GAGTGACATATGATTCGAGGTTATTGTTTGATGTAAATT
T2 (R)	CGCGTTGGGAAAACCCTTCTCGCCCATACATTCTATATC
Tet (F)	CATATGGCCGATTATGGTGCACTCTCAGTAC
Tet (R)	CATATGTGGTGAATCCGTTAGCGAGGTGCC

The protein complexes were immunoprecipitated with appropriate antibodies (anti-gB, anti-αV, or pre-immune IgG) for 1 h at 4 °C, followed by addition of 100 µl of swollen Protein A-Sepharose beads and further incubaton for another hour at 4 °C. The beads were washed four times with Gold lysis buffer, boiled in sample-loading buffer and resolved by 10 % SDS-PAGE gels. Proteins were transferred onto a PVDF membrane and Western blotted using appropriate antibodies as per previously described protocols (Akula *et al.*, 2002). The molecular masses of αV and α9 protein bands are 128 and 140 kDa, respectively.

Generating recombinant KSHV. A detailed protocol is provided in the online Supplementary Material.

Monitoring KSHV infection of cells. KSHV infection of different cells was recorded by counting the number of cells expressing GFP that is indicative of rKSHV.152 and BAC36 infection (Akula *et al.*, 2001b, 2004; Grange *et al.*, 2012).

Flow cytometry. Target cells were washed, incubated in growth medium at 37 °C for 30 min, centrifuged and resuspended in cold PBS. The entire procedure involved the use of cold reagents and temperatures of +4 °C. Cells (1×10^6) were incubated with different antibodies at 4 °C for 30 min, washed, incubated with FITC-conjugated appropriate secondary IgG at 4 °C for 30 min, washed and analysed in a FACScan flow cytometer (Becton Dickinson) with appropriate gating parameters.

ACKNOWLEDGEMENTS

We thank Dr Shou-Jiang (SJ) Gao (Keck School of Medicine, University of Southern California) to have graciously provided us with the BAC36 clone critical to this study. We also thank Dr Kumaran Narayanan (Monash University) to have kindly provided us with the pGET-rec plasmid, which again was a critical element of this project. Our sincere thanks go to Akarsh Manne and Dr Ivan Ndamukong for their assistance and guidance in generating recombinant viruses. Finally, we thank Frank Williams who performed quantitative real-time (qRT)-PCR for this study.

REFERENCES

Akula, S. M., Pramod, N. P., Wang, F. Z. & Chandran, B. (2001a). Human herpesvirus 8 envelope-associated glycoprotein B interacts with heparan sulfate-like moieties. *Virology* **284**, 235–249.

Akula, S. M., Wang, F. Z., Vieira, J. & Chandran, B. (2001b). Human herpesvirus 8 interaction with target cells involves heparan sulfate. *Virology* **282**, 245–255.

Akula, S. M., Pramod, N. P., Wang, F. Z. & Chandran, B. (2002). Integrin α3β1 (CD 49c/29) is a cellular receptor for Kaposi's sarcoma-associated herpesvirus (KSHV/HHV-8) entry into the target cells. *Cell* **108**, 407–419.

Akula, S. M., Ford, P. W., Whitman, A. G., Hamden, K. E., Shelton, J. G. & McCubrey, J. A. (2004). Raf promotes human herpesvirus-8 (HHV-8/KSHV) infection. *Oncogene* **23**, 5227–5241.

Akula, S. M., Ford, P. W., Whitman, A. G., Hamden, K. E., Bryan, B. A., Cook, P. P. & McCubrey, J. A. (2005). B-Raf-dependent expression of vascular endothelial growth factor-A in Kaposi sarcoma-associated herpesvirus-infected human B cells. *Blood* **105**, 4516–4522.

Andrews, M. R., Czvitkovich, S., Dassie, E., Vogelaar, C. F., Faissner, A., Blits, B., Gage, F. H., ffrench-Constant, C. & Fawcett, J. W. (2009). α9 integrin promotes neurite outgrowth on tenascin-C and enhances sensory axon regeneration. *J Neurosci* **29**, 5546–5557.

Backovic, M., Longnecker, R. & Jardetzky, T. S. (2009). Structure of a trimeric variant of the Epstein–Barr virus glycoprotein B. *Proc Natl Acad Sci U S A* **106**, 2880–2885.

Bryan, B. A., Dyson, O. F., McCubrey, J. A. & Akula, S. M. (2005). Biology of Kaposi's sarcoma-associated herpesvirus. *Front Biosci* **10**, 2882–2891.

Chakraborty, S., Veettil, M. V. & Chandran, B. (2012). Kaposi's sarcoma associated herpesvirus entry into target cells. *Front Microbiol* **3**, 6.

Chandran, B. (2010). Early events in Kaposi's sarcoma-associated herpesvirus infection of target cells. *J Virol* **84**, 2188–2199.

Chang, Y., Cesarman, E., Pessin, M. S., Lee, F., Culpepper, J., Knowles, D. M. & Moore, P. S. (1994). Identification of herpesvirus-like DNA sequences in AIDS-associated Kaposi's sarcoma. *Science* **266**, 1865–1869.

Desiderio, U. V., Zhu, X. & Evans, J. P. (2010). ADAM2 interactions with mouse eggs and cell lines expressing α4/α9 (ITGA4/ITGA9) integrins: implications for integrin-based adhesion and fertilization. *PLoS ONE* **5**, e13744.

Dyson, O. F., Traylen, C. M. & Akula, S. M. (2010). Cell membrane-bound Kaposi's sarcoma-associated herpesvirus-encoded glycoprotein B promotes virus latency by regulating expression of cellular Egr-1. *J Biol Chem* **285**, 37491–37502.

Dyson, O. F., Walker, L. R., Whitehouse, A., Cook, P. P. & Akula, S. M. (2012). Resveratrol inhibits KSHV reactivation by lowering the levels of cellular EGR-1. *PLoS ONE* **7**, e33364.

Eto, K., Huet, C., Tarui, T., Kupriyanov, S., Liu, H. Z., Puzon-McLaughlin, W., Zhang, X. P., Sheppard, D., Engvall, E. & Takada, Y. (2002). Functional classification of ADAMs based on a conserved motif for binding to integrin α9β1: implications for sperm-egg binding and other cell interactions. *J Biol Chem* **277**, 17804–17810.

Feire, A. L., Koss, H. & Compton, T. (2004). Cellular integrins function as entry receptors for human cytomegalovirus via a highly conserved disintegrin-like domain. *Proc Natl Acad Sci U S A* **101**, 15470–15475.

Feire, A. L., Roy, R. M., Manley, K. & Compton, T. (2010). The glycoprotein B disintegrin-like domain binds beta 1 integrin to mediate cytomegalovirus entry. *J Virol* **84**, 10026–10037.

Garrigues, H. J., Rubinchikova, Y. E., Dipersio, C. M. & Rose, T. M. (2008). Integrin αVβ3 binds to the RGD motif of glycoprotein B of Kaposi's sarcoma-associated herpesvirus and functions as an RGD-dependent entry receptor. *J Virol* **82**, 1570–1580.

Grange, P. A., Gressier, L., Williams, J. F., Dyson, O. F., Akula, S. M. & Dupin, N. (2012). Cloning a human saliva-derived peptide for preventing KSHV transmission. *J Invest Dermatol* **132**, 1733–1735.

Hahn, A., Birkmann, A., Wies, E., Dorer, D., Mahr, K., Stürzl, M., Titgemeyer, F. & Neipel, F. (2009). Kaposi's sarcoma-associated herpesvirus gH/gL: glycoprotein export and interaction with cellular receptors. *J Virol* **83**, 396–407.

Hahn, A. S., Kaufmann, J. K., Wies, E., Naschberger, E., Panteleev-Ivlev, J., Schmidt, K., Holzer, A., Schmidt, M., Chen, J. & other authors (2012). The ephrin receptor tyrosine kinase A2 is a cellular receptor for Kaposi's sarcoma-associated herpesvirus. *Nat Med* **18**, 961–966.

Hamden, K. E., Whitman, A. G., Ford, P. W., Shelton, J. G., McCubrey, J. A. & Akula, S. M. (2005). Raf and VEGF: emerging therapeutic targets in Kaposi's sarcoma-associated herpesvirus infection and angiogenesis in hematopoietic and nonhematopoietic tumors. *Leukemia* **19**, 18–26.

Inoue, N., Winter, J., Lal, R. B., Offermann, M. K. & Koyano, S. (2003). Characterization of entry mechanisms of human herpesvirus 8 by using an Rta-dependent reporter cell line. *J Virol* **77**, 8147–8152.

Laskowski, R. A., Gerick, F. & Thornton, J. M. (2009). The structural basis of allosteric regulation in proteins. *FEBS Lett* **583**, 1692–1698.

Lu, D., Scully, M., Kakkar, V. & Lu, X. (2010). ADAM-15 disintegrin-like domain structure and function. *Toxins (Basel)* **2**, 2411–2427.

Orend, G. & Chiquet-Ehrismann, R. (2006). Tenascin-C induced signaling in cancer. *Cancer Lett* **244**, 143–163.

Rappocciolo, G., Jenkins, F. J., Hensler, H. R., Piazza, P., Jais, M., Borowski, L., Watkins, S. C. & Rinaldo, C. R., Jr (2006). DC-SIGN is a receptor for human herpesvirus 8 on dendritic cells and macrophages. *J Immunol* **176**, 1741–1749.

Rappocciolo, G., Hensler, H. R., Jais, M., Reinhart, T. A., Pegu, A., Jenkins, F. J. & Rinaldo, C. R. (2008). Human herpesvirus 8 infects and replicates in primary cultures of activated B lymphocytes through DC-SIGN. *J Virol* **82**, 4793–4806.

Russo, J. J., Bohenzky, R. A., Chien, M. C., Chen, J., Yan, M., Maddalena, D., Parry, J. P., Peruzzi, D., Edelman, I. S. & other authors (1996). Nucleotide sequence of the Kaposi sarcoma-associated herpesvirus (HHV8). *Proc Natl Acad Sci U S A* **93**, 14862–14867.

Veettil, M. V., Sadagopan, S., Sharma-Walia, N., Wang, F. Z., Raghu, H., Varga, L. & Chandran, B. (2008). Kaposi's sarcoma-associated herpesvirus forms a multimolecular complex of integrins ($\alpha V\beta 5$, $\alpha V\beta 3$, and $\alpha 3\beta 1$) and CD98-xCT during infection of human dermal microvascular endothelial cells, and CD98-xCT is essential for the postentry stage of infection. *J Virol* **82**, 12126–12144.

Vieira, J., O'Hearn, P., Kimball, L., Chandran, B. & Corey, L. (2001). Activation of Kaposi's sarcoma-associated herpesvirus (human herpesvirus 8) lytic replication by human cytomegalovirus. *J Virol* **75**, 1378–1386.

Vlahakis, N. E., Young, B. A., Atakilit, A. & Sheppard, D. (2005). The lymphangiogenic vascular endothelial growth factors VEGF-C and -D are ligands for the integrin $\alpha 9\beta 1$. *J Biol Chem* **280**, 4544–4552.

Wang, F. Z., Akula, S. M., Sharma-Walia, N., Zeng, L. & Chandran, B. (2003). Human herpesvirus 8 envelope glycoprotein B mediates cell adhesion via its RGD sequence. *J Virol* **77**, 3131–3147.

Wolfsberg, T. G., Straight, P. D., Gerena, R. L., Huovila, A. P., Primakoff, P., Myles, D. G. & White, J. M. (1995). ADAM, a widely distributed and developmentally regulated gene family encoding membrane proteins with a disintegrin and metalloprotease domain. *Dev Biol* **169**, 378–383.

Yakushko, Y., Hackmann, C., Günther, T., Rückert, J., Henke, M., Koste, L., Alkharsah, K., Bohne, J., Grundhoff, A. & other authors (2011). Kaposi's sarcoma-associated herpesvirus bacterial artificial chromosome contains a duplication of a long unique-region fragment within the terminal repeat region. *J Virol* **85**, 4612–4617.

Yokosaki, Y., Palmer, E. L., Prieto, A. L., Crossin, K. L., Bourdon, M. A., Pytela, R. & Sheppard, D. (1994). The integrin alpha 9 beta 1 mediates cell attachment to a non-RGD site in the third fibronectin type III repeat of tenascin. *J Biol Chem* **269**, 26691–26696.

Young, B. A., Taooka, Y., Liu, S., Askins, K. J., Yokosaki, Y., Thomas, S. M. & Sheppard, D. (2001). The cytoplasmic domain of the integrin $\alpha 9$ subunit requires the adaptor protein paxillin to inhibit cell spreading but promotes cell migration in a paxillin-independent manner. *Mol Biol Cell* **12**, 3214–3225.

Zhang, W. & Gao, S. J. (2012). Exploitation of cellular cytoskeletons and signaling pathways for cell entry by Kaposi's sarcoma-associated herpesvirus and the closely related rhesus rhadinovirus. *Pathogens* **1**, 102–127.